The Cryosphere Discuss., 9, 4865–4892, 2015
www.the-cryosphere-discuss.net/9/4865/2015/
doi:10.5194/tcd-9-4865-2015

The Cryosphere Discussions
Open Access

Glacier dynamics over the last quarter of a century at Jakobshavn Isbræ

I. S. Muresan[1], S. A. Khan[1], A. Aschwanden[2], C. Khroulev[2], T. Van Dam[3], J. Bamber[4], M. R. van den Broeke[5], B. Wouters[4], P. Kuipers Munneke[5], and K. H. Kjær[6]

[1]Department of Geodesy, DTU Space, Technical University of Denmark, Kgs. Lyngby, Denmark
[2]Geophysical Institute, University of Alaska Fairbanks, Fairbanks, Alaska, USA
[3]University of Luxembourg, Faculty of Science, Technology and Communication (FSTC), Engineering Research Unit, Luxembourg
[4]University of Bristol, School of Geographical Sciences, Bristol, UK
[5]Institute for Marine and Atmospheric research Utrecht (IMAU), Utrecht University, Utrecht, the Netherlands
[6]Centre for GeoGenetics, Natural History Museum of Denmark, University of Copenhagen, Copenhagen, Denmark

Received: 20 August 2015 – Accepted: 28 August 2015 – Published: 14 September 2015

Correspondence to: I. S. Muresan (iomur@space.dtu.dk)

Published by Copernicus Publications on behalf of the European Geosciences Union.

Abstract

Observations over the past two decades show substantial ice loss associated with the speedup of marine terminating glaciers in Greenland. Here we use a regional 3-D outlet glacier model to simulate the behaviour of Jakobshavn Isbræ (JI) located in west Greenland. Using atmospheric and oceanic forcing we tune our model to reproduce the observed frontal changes of JI during 1990–2014. We identify two major accelerations. The first occurs in 1998, and is triggered by moderate thinning prior to 1998. The second acceleration, which starts in 2003 and peaks in summer 2004, is triggered by the final breakup of the floating tongue, which generates a reduction in buttressing at the JI terminus. This results in further thinning, and as the slope steepens inland, sustained high velocities have been observed at JI over the last decade. As opposed to other regions on the Greenland Ice Sheet (GrIS), where dynamically induced mass loss has slowed down over recent years, both modelled and observed results for JI suggest a continuation of the acceleration in mass loss. Further, we find that our model is not able to capture the 2012 peak in the observed velocities. Our analysis suggests that the 2012 acceleration of JI is likely the result of an exceptionally long melt season dominated by extreme melt events. Considering that such extreme surface melt events are expected to intensify in the future, our findings suggest that the 21st century projections of the GrIS mass loss and the future sea level rise may be larger than predicted by existing modelling results.

1 Introduction

The rate of ice mass loss from Greenlandic marine terminating glaciers has more than doubled over the past two decades (Rignot et al., 2008; Moon et al., 2012; Shepherd et al., 2012). Jakobshavn Isbræ is the largest outlet glacier in terms of drainage area as it drains ~ 6 % of the GrIS (Krabill et al., 2000). Due to its consistently high flow rate and seasonally varying rate of flow and front position, the glacier has received much attention in the last two decades (Thomas et al., 2003; Luckman and Murray, 2005; Holland et al., 2008; Amundson et al., 2010; Khan et al., 2010; Motyka et al., 2011; Joughin et al., 2012; Gladish et al., 2015b, a). Measurements from synthetic aperture radar suggest that the speed of JI doubled between 1992 and 2003 (Joughin et al., 2004). More recent measurements show a steady increase in the flow rate over the glacier's faster-moving region of $\sim 5\,\%\,\text{year}^{-1}$ (Joughin et al., 2008). The speedup coincides with thinning of up to $15\,\text{m}\,\text{a}^{-1}$ between 2006 and 2012 near the glacier front (Nielsen et al., 2013) as observed from airborne laser altimeter surveys. The steady increase in the flow rate and glacier thinning suggest a continuous dynamic drawdown of mass, and highlights JIs importance for predicting present and future sea level rise.

In general, reproducing past and present-day observations of the dynamical behaviour of Greenland's outlet glaciers is the key for developing realistic projections of future changes in the GrIS (IPCC, 2013). The past decade has shown significant improvements in the numerical modelling of glaciers and ice sheets (e.g. Price et al., 2011; Vieli and Nick, 2011; Winkelmann et al., 2011; Larour et al., 2012; Pattyn et al., 2012; Seroussi et al., 2012; Aschwanden et al., 2013; Nick et al., 2013; Mengel and Levermann, 2014). Some regional scale glacier models are based on a flow-line approach (Nick et al., 2009; Parizek and Walker, 2010), which models the one- or two-dimensional dynamic behaviour of the glacier under consideration. Flow-line models are computationally efficient and valuable for understanding basic processes. However, three-dimensional models are more appropriate in areas of flow divergence/convergence and/or where lateral stresses are important.

In the last decade, several processes have been identified to control the observed speedup at JI (Nick et al., 2009; Van der Veen et al., 2011; Joughin et al., 2012). One is a reduction in resistance (buttressing) at the marine front through thinning or retreat of the floating tongue of the glacier, but the details of the processes triggering and controlling thinning and retreat remain elusive. Accurately modelling complex interactions between thinning, retreat, and acceleration as observed at JI, is challenging. Our knowledge of the mechanisms triggering these events is usually constrained to the period covered by observations. The initial speedup of JI occurred during the time when the satellite and airborne observations were infrequent and therefore insufficient to monitor the seasonal to monthly evolution of glacier geometry and speed.

In this paper, a high-resolution, three dimensional and time-dependent regional outlet glacier model, developed as part of the Parallel Ice Sheet Model (PISM; please refer to Sect. 2.1 The ice sheet model) (The PISM Authors, 2014), is used to investigate the processes driving the dynamic evolution and the seasonal velocity variation of JI between 1990–2014. The period prior to 2004 is characterized by sparsely sampled data with observations available only during 1992, 1995 and between 2000 and 2003. The second part of 2003 and the first part of 2004 are missing entirely from the available observational record (Joughin et al., 2008, 2012). Therefore, we concentrate our efforts on resolving the degree of seasonal velocity variation before, during, and after the final breakup of the ice tongue in the summer of 2003 (Luckman and Murray, 2005; Joughin et al., 2008). Our modelling approach is based on a regional equilibrium run and a time-integration from 1990 to 2014 where the grounding lines and the calving fronts are free to evolve under monthly climatic forcing and oceanic boundary conditions.

2 Methods

2.1 The ice sheet model

The ice sheet model used in this study is PISM (stable version 0.6). PISM is an open source, parallel, three-dimensional, thermodynamically coupled and time dependent ice sheet model (Bueler and Brown, 2009; Winkelmann et al., 2011; The PISM Authors, 2014). The ice dynamic model is the "SIA+SSA hybrid", with the non-sliding shallow ice approximation (SIA) for simulating slowly moving grounded ice in the interior part of the ice sheet and the shallow shelf approximation (SSA) for simulating fast-flowing outlet glacier and ice shelf systems (Bueler and Brown, 2009). The superposition of SIA and SSA sustains a smooth transition between non-sliding, bedrock frozen ice and sliding, fast-flowing ice, and it is known to reasonably capture the fast moving grounded ice (Winkelmann et al., 2011). For conservation of energy, PISM uses an enthalpy scheme that accounts for the latent heat content within temperate ice (i.e., ice at the pressure melting point) (Aschwanden et al., 2012).

We start our regional JI runs with an equilibrium simulation on a 125 × 86 horizontal grid with 5 km spacing and a vertical resolution of 20 m. The enthalpy formulation models the mass and energy balance for the three dimensional ice fluid field based on 200 regularly spaced layers within the ice in a computational domain that does not extend farther than 4000 m above the bed. The temperature in the bedrock thermal layer is computed up to a depth of 1000 m with 50 regularly spaced layers. The first step is to obtain a 5 km regional equilibrium model for JI using constant mean climate (i.e. repeating the 1960–1990 mean air temperature and surface mass balance; see 2.1.1 Input data). We consider that equilibrium has been established when the ice volume in the regional domain changes by less than 1 % in the final 100 model years. Grid refinements are made from 5 km (125 × 86) to 2 km (310 × 213) after 3000 years. The length of the simulation with the 2 km grid is 200 years. The model reaches equilibrium with an ice volume of 0.25 (10^6 km^3) (or a 3.6 % increase relative to the input dataset from Bamber et al. (2013) adjusted to simulate 1990's metrics) and horizontal velocities that do not exceed 5500 m a^{-1} near the terminus. By the end of the equilibrium simulation, thin ice (< 400 m) fills the ice fjord up to 2 to 4 km away from the 1990 observed frontal position. This excess thin ice is calved within the first two years of the forward simulation. Using our equilibrium simulations with 2 km and with a 10 m grid in vertical, we integrate forward in time (hindcast) from 1990 to 2014 by imposing monthly fields of SMB and 2 m air temperatures through a one-way coupling scheme. The calving fronts and grounding lines are free to evolve in time both during the equilibrium and the forward simulation (see 2.1.2 Boundary conditions, calving and ground line parametrization).

TCD
9, 4865–4892, 2015

2.1.1 Input data

The bed topography used in this study is from Bamber et al. (2013). The bed elevation dataset for all of Greenland has a 1 km spatial resolution and was derived from a combination of multiple airborne ice thickness surveys and satellite-derived elevations undertaken between 1970–2012 (Bamber et al., 2013). The terminus position and surface elevation in the Jakobshavn region is further adjusted to simulate 1990's metrics based on 1985 aerial photographs and existing satellite altimetry observations (Csatho et al., 2008). Ice thickness in the JI basin is computed as the difference between surface and bedrock elevation, which implies that at the beginning of our equilibrium simulation JI's terminus is considered grounded. The model of the geothermal flux is from Shapiro and Ritzwoller (2004). The input fields of near-surface air temperature and surface mass balance are from the regional climate model RACMO2.3 (Noël et al., 2015). The version used in this study is produced at a spatial resolution of ~ 11 km and is extended to the end of 2014, to cover the period 1958–2014.

2.1.2 Boundary conditions, calving and ground line parametrization

In the regional outlet glacier model of PISM, the boundary conditions are handled in a 10 km strip positioned outside of the JI's drainage basin and around the edge of the computational domain. In this strip, the input values of the basal melt, the amount of till-pore water, ice enthalpy, and lithospheric temperature (Aschwanden et al., 2013) are held fixed and interpreted as Dirichlet boundary conditions by the conservation of energy model (The PISM Authors, 2014). In our model, the three-dimensional ice enthalpy field, basal melt, modelled amount of till-pore water, and lithospheric temperature are given as simulated in a whole GrIS paleo-climatic spin-up. The paleo-climatic spin-up follows closely the initialization procedure described in detail by Bindschadler et al. (2013) and Aschwanden et al. (2013). Along the ice shelf calving front, we apply a physically based calving (eigencalving) parametrization (Winkelmann et al., 2011; Levermann et al., 2012) and an ice thickness condition (Albrecht et al., 2011). The calving law is known to yield realistic calving front positions for various types of ice shelves being successfully used for modelling calving front positions in whole Antarctica simulations (Martin et al., 2011) and regional east Antarctica simulations (Mengel and Levermann, 2014). The calving fronts and grounding lines are free to evolve in time. The parameterization of the grounding line position is based on the "LI" parameterization (Gladstone et al., 2010). In the Mismip3d experiments, PISM was used to model reversible grounding line dynamics with results consistent with full-Stokes models (Feldmann et al., 2014).

2.1.3 Ocean model component

We use an ocean model component where the melting effect of the ocean is based on both sub-shelf ocean temperature and salinity (Martin et al., 2011). The sub-shelf ice temperature is set to the pressure-melting temperature being applied as a Dirichlet boundary condition in the conservation of energy equation, while the mass flux from shelf to ocean applied follows Beckmann and Goosse (2003). This mass flux is computed as a heat flux between the ocean and ice that represents the melting effect of the ocean through both temperature and salinity (Martin et al., 2011). We start our simulations with a constant ocean water temperature of $-1.7\,^{\circ}\mathrm{C}$ which is further scaled in the ocean-ice boundary layer spatially and temporally based on the ocean water salinity and on the depth below the ice shelf (see Eqs. 4 and 5 from Martin et al. (2011) and Table S1 for their respective values). Therefore, the sub-shelf melt rates are dependent on the ice shelf thickness. We choose to keep the ocean water salinity constant in time and space (see Table S1) as the model does not capture the salinity gradient from the base of the ice shelf through layers of low and high salinity. However, a previous study conducted by Mengel and Levermann (2014) using the same model established that the sensitivity of the melt rate to salinity is negligible.

TCD
9, 4865–4892, 2015

3 Results and discussion

Fifty simulations are performed with different sets of parameters. From these results, we present here the parameterization that best captures the full evolution of JI during the period 1990–2014 (see Sect. S1 for more details and for the values of the ice sheet model parameters and Sect. 5 for the evolution of the main driver variables for the atmosphere and the ocean).

3.1 Observations vs. modelling results

We calibrated the parameters such that the model reproduces the frontal positions (Fig. 2) and the ice mass change observations (Fig. 4, please refer to Sect. 3.1.1 Mass change) at JI during the period 1990–2014 and 1997–2014, respectively. The procedure for deriving the observed ice mass change is described in Sect. S2. In order to match the observed front positions a sub-shelf melting parameter (F_{melt}) with a value of 0.198 $\mathrm{m\,s^{-1}}$ (see Eq. 5 from Martin et al., 2011) is used in our simulations and results in basal melt rates slightly larger than those obtained by Motyka et al. (2011).

When the modelled velocities in the points S1 to S7 (Fig. 1) are compared with available observations from Smith et al. (2010) the model is able to reproduce the overall pattern of the observed velocities. However, the modelled velocity at point S4 is underestimated and at point S7 is overestimated. Further for all the points and all the simulations the model does not capture the anomalous 2012 observed velocities (see Fig. 3).

A previous analysis by Joughin et al. (2014) attributes the acceleration and the summer peak of 2012 to the retreat of the JI terminus to the bottom of an over deepened basin (see Fig. 3 from Joughin et al., 2014). This retreat, which started in 2009 (Joughin et al., 2014), should have triggered an acceleration of JI as soon as the terminus started to retreat in 2009 over the slope of the over deepened basin. However, there is no evidence of such acceleration either in the observational record (see Fig. 1 from Joughin et al., 2014), nor in our simulations (see Figs. 3 and 6 and Sect. 3.2,

TCD
9, 4865–4892, 2015

2003–2014 for more details). Furthermore, the summer of 2012 is characterized by exceptional surface melt, covering 98 % of the entire ice sheet surface, including the high altitude Summit region (Nghiem et al., 2012; Hanna et al., 2014). The three extreme melt events that occurred between 10 July and 10 August 2012 (see Fig. 1a from Hanna et al., 2014, and Fig. 3 from NSIDC, 2015) might have enhanced hydrofracturing of the calving front due to melt draining into surface crevasses (MacAyeal et al., 2003; Joughin et al., 2013; Pollard et al., 2015) resulting in greater and/or faster seasonal retreat and increase the submarine melt at the terminus and the sub-shelf cavity (Schoof, 2007; Stanley et al., 2011; Kimura et al., 2014; Slater et al., 2015), which likely triggered the rapid acceleration in the observed ice surface speed in the summer of 2012. Overall, the 2012 melt-season was two months longer than the 1979–2011 mean and the longest recorded in the satellite era (Tedesco et al., 2013). An intense and long melt year leads to strong thinning of the ice, steepening surface slopes, and has the potential to further sustain the initial acceleration of JI through enhanced longitudinal stretching. Furthermore, a study by Doyle et al. (2015) found that during an amplified melt event (caused by late-summer cyclonic rainfall that occurred between 23 August and 3 September 2011) JIs speed increased by 10 % (see Fig. S3 in Doyle et al., 2015). Therefore, the influence of enhanced surface melting in JIs dynamics has been proven. Under normal circumstances (i.e. average melt years), the winter slowdown is usually able to compensate for the summer acceleration events. The summer of 2012 was however preceded by a series of warm summers (2007, 2008, 2010 and 2011) (Hanna et al., 2014), which may have created the conditions under which the winter slowdowns can no longer compensate for the summer accelerations leading to an increase in the mean annual flow. Bougamont et al. (2014) showed that a sustained increase in surface runoff by 50 % may cause some small runoff events to increase ice flow magnitudes to those observed in individual supraglacial lake drainage events. To account for the influence of meltwater runoff and its role in the subglacial system during such extreme melt events in modelling simulations only by means of inputs from climate models, is very challenging. There have been very few observational studies of meltwater runoff through supraglacial water storage, drainage, and discharge patterns and therefore these events cannot be represented nor captured accurately by current ice sheet models without any additional coupling. Failing to accurately represent these processes may lead to an underestimation of the flow speed during intense melt events as observed in our simulations (Fig. 3, year 2012).

3.1.1 Mass change

Figure 4 shows observed and modelled mass change for the period 1997 to 2014. We estimate the rate of ice volume change from airborne and satellite altimetry over the same period and convert to mass change rate (see Sect. S2). Overall there is good agreement between modelled and observed mass change over this period (see Fig. 4), and our results are in agreement with other similar studies (Howat et al., 2011; Nick et al., 2013). Dynamically driven discharge is known to control Jakobshavn's mass loss (Nick et al., 2013). The modelled cumulative mass loss is 269 Gt, of which 93 % (∼ 251 Gt) is determined to be dynamic in origin while the remaining 7 % (∼ 18 Gt) is attributed to a decrease in SMB (see Fig. 4). Further, the present-day unloading of ice causes the Earth to respond elastically. Thus, we can use modelled mass changes to predict elastic uplift. We compare modelled changes of the Earth's elastic response to changes in ice mass to uplift observed at four GPS sites (see Fig. 5 and Sect. S3). Both model and observations consistently suggest large uplift near the JI front and somewhat minor uplift rates of few $\mathrm{mm\,a^{-1}}$ at distances of > 100 km from the ice margin.

3.2 Seasonal variations in velocities

We investigate the processes driving the dynamic evolution of JI and its seasonal variation in velocity between 1990–2014 with a focus on the initial speedup of JI and the 2003 breakup of the ice tongue. The pattern observed in our simulations suggests a gradual increase in velocities that agrees well with observations (Joughin et al., 2008;

Smith et al., 2010; Joughin et al., 2014) (Fig. 3). Three distinct stages of acceleration are identified in Fig. 3 (see also Movie 1) and discussed in detail below.

– **1990–1997**

The first period of acceleration is caused by a retreat of the front position by approximately 2 to 4 km between 1990 and 1991. There is no observational evidence that this retreat actually occurred. It is probably a modelling artefact as the geometry obtained during the regional equilibrium simulation is forced with new oceanic and atmospheric conditions. During the first two years, 1990–1991, the model is still calving the excess thin ice (< 400 m) generated during the equilibrium simulation. This acceleration results from a reduction in resistive stress near the grounding line, generated by the gradual retreat of the front, triggering a dynamic response in the upstream region of JI.

Starting in 1992 we obtain a good fit of our model to the observed frontal positions. Disregarding the acceleration observed in 1991–1992, no significant seasonal fluctuation in flow rate is observed during this period. Beginning in 1993, a stronger seasonal velocity signal begins to emerge in our simulation that continues and intensifies in magnitude during 1994 and 1995. In 1996 and 1997, the frontal extent and the grounding line position remain relatively stable (Figs. 2 and 6), and no significant seasonal fluctuation in flow rate is observed. These model results agree well with observations, which indicate that the glacier speed was relatively constant during this period (Joughin et al., 2004; Luckman and Murray, 2005).

– **1998–2002**

According to observations (Joughin et al., 2004; Motyka et al., 2011; Bevan et al., 2012), the initial acceleration of JI occurred in May–August 1998, which coincides with our modelling results. In our simulation, the 1998 acceleration is generated by an increase in surface slopes due to thinning both near the terminus and inland (up to 10 km away from the 1990 front position). These findings are corroborated both by observations (Fig. S1) and modelling results (Fig. 6). The thinning starts in our model in the summer of 1995 and continues to accelerate after 1998 (Figs. 3 and 6). In addition, a small retreat can be observed on the north side of the fjord, which may be responsible for a reduction in lateral shear (see Movie 1). We observe a retreat of the grounding line position starting in 1998 that accelerates thereafter (Figs. 2 and 6). Although thinning appears to have increased in our model during three continuous years we find little additional speedup during the period prior to 1998 (Figs. 2 and 6). According to our simulation, JI's speed increased in the summer of 1998 by ∼ 80 % relative to the summer of 1992 (Fig. 3). We attribute most of the observed 1998 acceleration to a reduction in lateral stress, retreat of the grounding line, and a thinning of the southern tributary that characterized JI from 1995 to 1998. The period between 1999 and 2002 is in our simulation characterized by a temporally uniform flow, with no episodes of significant retreat. Overall we observe an advance of the terminus between 1999 and 2000 and a retreat of the southern tributary between 2000 and 2002 by ∼ 2 km, which correlates with existing observations (Thomas, 2004). Concurrent with the 1998–2001 terminus retreat, the grounding line retreats in our model by ∼ 4 km. The grounding line retreat sustained by the bed geometry (Figs. 2 and 6) is further combined with calving and thinning near the front and results in a reduction of resistive stresses at the terminus.

– **2003–2014**

In the late summer of 2003, a steep increase in flow velocity can be observed in Fig. 3, which is driven in our simulations by the final breakup of the ice tongue (see Figs. 2 and 6). The period 2002–2003 is characterized by substantial retreat of the front (∼ 4–6 km) and the grounding line (∼ 4 km), which starts in June 2002 and continues throughout 2003. By December 2003 the terminus has retreated back to the position of the grounding line (see Figs. 2 and 6). In our simulation, the retreat that occurred in 2003 and the loss of much of the floating tongue causes a major decrease in resistive stresses near the terminus. By 2004 the glacier has thinned significantly both near the front and further inland in response to a change in the near-terminus stress field (Figs. 3 and 6). During the ice tongue final breakup, JI reached unprecedented flow rates, which in our simulation are as high as $20\,\mathrm{km\,a^{-1}}$ ($\sim 120\,\%$ increase relative to 1998). The velocities decrease to $16\,\mathrm{km\,a^{-1}}$ ($\sim 80\,\%$ increase relative to 1998) in the subsequent months, and JI remains relatively stable with high seasonal fluctuations. The high velocities observed at JI after the loss of its floating tongue are further sustained in our simulation by the thinning that occurred in 2004 onward (see Fig. 3) and which continues to steepen the slopes near the terminus (see Fig. 6). This thinning is combined in the following years with a reduction in surface mass balance due to increased melting and runoff (van den Broeke et al., 2009; Enderlin et al., 2014; Khan et al., 2014). The period 2004–2014 is characterized in our simulation by relatively uniform velocities with strong seasonal variations (Fig. 3). During this period, the terminus remains close to the grounding line position with no episodes of significant retreat.

In contrast to other drainage basins of the GrIS where the mass loss and flow speed slowed down in recent years (Khan et al., 2010; Bevan et al., 2012; Enderlin et al., 2014), in the Jakobshavn basin both modelled and observed data suggest that the JI continued to loose mass at an accelerated rate between 2013–2014.

4 Conclusions

A three dimensional, time-dependent regional outlet glacier model is used to investigate the processes driving the dynamic evolution of JI and its seasonal variation in velocity between 1990 and 2014. The model parameters were calibrated such that the model reproduces the frontal positions observed at JI during the period 1990–2014. We obtain a good agreement of our model output with measured horizontal velocities, observed mass change, and GPS derived uplift (Figs. 3–5).

We find that our model is not able to simulate the 2012 spike in flow velocity observed at JI, however, we are able to capture the overall trend in the observed velocities (Fig. 3). The acceleration that characterizes JI during 2012 is likely the result of an exceptionally long melting season dominated by extreme melt events (Nghiem et al., 2012; Tedesco et al., 2013; Hanna et al., 2014) and may not be caused by a retreat of the JI terminus to the bottom of an overdeepened basin (Joughin et al., 2014). Modelling the influence of surface processes in flow acceleration only by means of input data from climate models and without an adequate account of supraglacial water storage, drainage, and discharge patterns as well as their impact on flow, results in models that are not able to capture the acceleration caused by such intense melt events. Considering that the GrIS is highly sensitive to changes in the regional and global climate and that such events are expected to intensify in the future (Keegan et al., 2014), our findings suggest that current projections of 21st century mass loss may be underestimated.

Our model results provide evidence for two distinct flow accelerations in 1998 and 2003, respectively. The first was generated by an increase in surface slope and thinning prior to 1998; the latter was triggered by the final breakup of the floating tongue. During this period, JI attained unprecedented velocities as high as 20 $\mathrm{km\,a^{-1}}$. Additionally, the final breakup of the floating tongue generated a reduction in buttressing that resulted in further thinning. As the slope steepened inland, sustained high flow rates have been observed at JI over the last decade. In accordance with previous studies (Thomas, 2004; Joughin et al., 2012), our findings suggest that the speed observed today at JI is a result of thinning induced changes and a reduction in resistive stress (buttressing) near the terminus correlated with inland steepening slopes.

Furthermore, despite the slow-down of glacier speed in other drainage basins of the GrIS over recent years (Bevan et al., 2012; Enderlin et al., 2014), our modelled and observed results suggest that JI has been losing mass at an accelerated rate, and it continued to accelerate through 2014 when other glaciers slowed (Fig. 4).

TCD
9, 4865–4892, 2015

The Supplement related to this article is available online at doi:10.5194/tcd-9-4865-2015-supplement.

Acknowledgements. Ioana S. Muresan is funded by the Forskningsraadet for Natur og Univers (FNU). Shfaqat A. Khan is partially supported by Carlsbergfondet. Bert Wouters is funded by a Marie Curie International Outgoing Fellowship within the 7th European Community Framework Programme (FP7-PEOPLE-2011-IOF-301260). The development of PISM is supported by NASA grants NNX13AM16G and NNX13AK27G. We thank Veit Helm for providing cryosat-2 data.

References

Albrecht, T., Martin, M., Haseloff, M., Winkelmann, R., and Levermann, A.: Parameterization for subgrid-scale motion of ice-shelf calving fronts, The Cryosphere, 5, 35–44, doi:10.5194/tc-5-35-2011, 2011.

Amundson, J. M., Fahnestock, M., Truffer, M., Brown, J., Lüthi, M. P., and Motyka, R. J.: Ice mélange dynamics and implications for terminus stability, Jakobshavn Isbræ, Greenland, J. Geophys. Res., 115, F01005, doi:10.1029/2009JF001405, 2010.

Aschwanden, A., Bueler, E., Khroulev, C., and Blatter, H.: An enthalpy formulation for glaciers and ice sheets, J. Glaciol., 58, 441–457, doi:10.3189/2012JoG11J088, 2012.

Aschwanden, A., Aðalgeirsdóttir, G., and Khroulev, C.: Hindcasting to measure ice sheet model sensitivity to initial states, The Cryosphere, 7, 1083–1093, doi:10.5194/tc-7-1083-2013, 2013.

Bamber, J. L., Griggs, J. A., Hurkmans, R. T. W. L., Dowdeswell, J. A., Gogineni, S. P., Howat, I., Mouginot, J., Paden, J., Palmer, S., Rignot, E., and Steinhage, D.: A new bed elevation dataset for Greenland, The Cryosphere, 7, 499–510, doi:10.5194/tc-7-499-2013, 2013.

Beckmann, A. and Goosse, H.: A parameterization of ice shelf–ocean interaction for climate models, Ocean Model., 5, 157–170, doi:10.1016/S1463-5003(02)00019-7, 2003.

Bevan, S. L., Luckman, A. J., and Murray, T.: Glacier dynamics over the last quarter of a century at Helheim, Kangerdlugssuaq and 14 other major Greenland outlet glaciers, The Cryosphere, 6, 923–937, doi:10.5194/tc-6-923-2012, 2012.

Bindschadler, R. A., Nowicki, S., Abe-Ouchi, A., Aschwanden, A., Choi, H., Fastook, J., Granzow, G., Greve, R., Gutowski, G., Herzfeld, U., Jackson, C., Johnson, J., Khroulev, C., Levermann, A., Lipscomb, W. H., Martin, M. A., Morlighem, M., Parizek, B. R., Pollard, D., Price, S. F., Ren, D., Saito, F., Sato, T., Seddik, H., Seroussi, H., Takahashi, K., Walker, R., and Wang, W. L.: Ice-Sheet Model Sensitivities to Environmental Forcing and Their Use in Projecting Future Sea Level (the SeaRISE Project), J. Glaciol., 59, 195–224, doi:10.3189/2013JoG12J125, 2013.

Bougamont, M., Christoffersen, P., Hubbard, A. L., Fitzpatrick, A. A., Doyle, S. H., and Carter, S. P.: Sensitive response of the Greenland Ice Sheet to surface melt drainage over a soft bed, Nature Comm., 5, 5052, doi:10.1038/ncomms6052, 2014.

Bueler, E. and Brown, J.: Shallow shelf approximation as a "sliding law" in a thermodynamically coupled ice sheet model, J. Geophys. Res., 114, F03008, doi:10.1029/2008JF001179, 2009.

Csatho, B., Schenk, T., Van Der Veen, C. J., and Krabill, W. B.: Intermittent thinning of Jakobshavn Isbræ, West Greenland, since the Little Ice Age, J. Glaciol., 54, 131–144, doi:10.3189/002214308784409035, 2008.

Doyle, S. H., Hubbard, A., van de Wal, R. S. W., Box, J. E., van As, D., Scharrer, K., Meierbachtol, T. W., Smeets, P. C. J. P., Harper, J. T., Johansson, E., Mottram, R. H., Mikkelsen, A. B., Wilhelms, F., Patton, H., Christoffersen P., and Hubbard, B.: Amplified melt and flow of the Greenland ice sheet driven by late-summer cyclonic rainfall, Nat. Geosci., 8, 647–653, doi:10.1038/ngeo2482, 2015.

Enderlin, E. M., Howat, I. M., Jeong, S., Noh, M. J., van Angelen, J. H., and van den Broeke, M. R.: An improved mass budget for the Greenland ice sheet, Geophys. Res. Lett., 41, 866–872, doi:10.1002/2013GL059010, 2014.

Feldmann, J., Albrecht, T., Khroulev, C., Pattyn, F., and Levermann, A.: Resolution-dependent performance of grounding line motion in a shallow model compared with a full-Stokes model according to the MISMIP3d intercomparison, J. Glaciol., 60, 353–360, doi:10.3189/2014JoG13J093, 2014.

Gladish, C. V., Holland, D. M., and Lee, C. M.: Oceanic boundary conditions for Jakobshavn Glacier. Part II: Provenance and sources of variability of Disko Bay and Ilulissat icefjord waters, 1990–2011, J. Phys. Oceanogr., 45, 33–63, doi:10.1175/JPO-D-14-0045.1, 2015a.

Gladish, C. V., Holland, D. M., Rosing-Asvid, A., Behrens, J. W., and Boje, J.: Oceanic boundary conditions for Jakobshavn Glacier. Part I: Variability and renewal of Ilulissat icefjord waters, 2001–2014, J. Phys. Oceanogr., 45, 3–32, doi:10.1175/JPO-D-14-0044.1, 2015b.

Gladstone, R. M., Payne, A. J., and Cornford, S. L.: Parameterising the grounding line in flow-line ice sheet models, The Cryosphere, 4, 605–619, doi:10.5194/tc-4-605-2010, 2010.

Hanna, E., Fettweis, X., Mernild, S., Cappelen, J., Ribergaard, M., Shuman, C., Steffen, K., Wood, L., and Mote, T.: Atmospheric and oceanic climate forcing of the exceptional Greenland ice sheet surface melt in summer 2012, Int. J. Climatol., 34, 1022–1037, doi:10.1002/joc.3743, 2014.

Holland, D. M., Thomas, R. H., de Young, B., Ribergaard, M. H., and Lyberth, B.: Acceleration of Jakobshavn Isbræ triggered by warm subsurface ocean waters, Nat. Geosci., 1, 659–664, doi:10.1038/ngeo316, 2008.

Howat, I. M., Ahn, Y., Joughin, I., van den Broeke, M. R., Lenaerts, J. T. M., and Smith, B.: Mass balance of Greenland's three largest outlet glaciers, 2000–2010, Geophys. Res. Lett., 38, L12501, doi:10.1029/2011GL047565, 2011.

IPCC: Climate Change 2013: the Physical Science Basis, contribution of Working Group I to the Fifth Assessment Report of the Intergovernmental Panel on Climate Change, Cambridge University Press, Cambridge, UK and New York, NY, USA, 1535 pp., doi:10.1017/CBO9781107415324, 2013.

Joughin, I., Abdalati, W., and Fahnestock, M.: Large fluctuations in speed on Greenland's Jakobshavn Isbræ glacier, Nature, 432, 608–610, doi:10.1038/nature03130, 2004.

Joughin, I., Howat, I. M., Fahnestock, M., Smith, B., Krabill, W., Alley, R. B., Stern, H., and Truffer, M.: Continued evolution of Jakobshavn Isbrae Following Its Rapid Speedup, J. Geophys. Res., 113, F04006, doi:10.1029/2008JF001023, 2008.

Joughin, I, Smith, B. E., Howat, I. M., Scambos, T., and Moon, T.: Greenland flow variability from ice–sheet–wide velocity mapping, J. Glaciol., 56, 415–430, doi:10.3189/002214310792447734, 2010.

Joughin, I., Howat, I., Smith, B., and Scambos, T.: MEaSUREs Greenland Ice Velocity: Selected Glacier Site Velocity Maps from InSAR, NASA DAAC at the National Snow and Ice Data Center, Boulder, Colorado, USA, doi:10.5067/MEASURES/CRYOSPHERE/nsidc-0481.001, 2011.

Joughin, I., Smith, B. E., Howat, I. M., Floricioiu, D., Alley, R. B., Truffer, M., and Fahnestock, M.: Seasonal to decadal scale variations in the surface velocity of Jakobshavn Isbræ, Greenland: observation and model-based analysis, J. Geophys. Res., 117, F02030, doi:10.1029/2011JF002110, 2012.

TCD
9, 4865–4892, 2015
Glacier dynamics over the last quarter of a century at Jakobshavn Isbræ
I. S. Muresan et al.

Joughin, I., Das, S. B., Flowers, G. E., Behn, M. D., Alley, R. B., King, M. A., Smith, B. E., Bamber, J. L., van den Broeke, M. R., and van Angelen, J. H.: Influence of ice-sheet geometry and supraglacial lakes on seasonal ice-flow variability, The Cryosphere, 7, 1185–1192, doi:10.5194/tc-7-1185-2013, 2013.
Joughin, I., Smith, B. E., Shean, D. E., and Floricioiu, D.: Brief Communication: Further summer speedup of Jakobshavn Isbræ, The Cryosphere, 8, 209–214, doi:10.5194/tc-8-209-2014, 2014.
Keegan, K. M., Albert, R. M., McConnell, J. R., and Baker, I.: Climate change and forest fires synergistically drive widespread melt events of the Greenland Ice Sheet, P. Natl. Acad. Sci. USA, 111, 7964–7967, doi:10.1073/pnas.1405397111, 2014.
Khan, S. A., Liu, L., Wahr, J., Howat, I., Joughin, I., van Dam, T., and Fleming, K.: GPS measurements of crustal uplift near Jakobshavn Isbræ due to glacial ice mass loss, J. Geophys. Res., 115, B09405, doi:10.1029/2010JB007490, 2010.
Khan, S. A., Kjær, K. H., Bevis, M., Bamber, J. L., Wahr, J., Kjeldsen, K. K., Bjørk, A. A., Korsgaard, N. J., Stearns, L. A., van den Broeke, M. R., Liu, L., Larsen, N. K., and Muresan, I. S.: Sustained mass loss of the Northeast Greenland ice sheet triggered by regional warming, Nature Clim. Change, 4, 292–299, doi:10.1038/nclimate2161, 2014.
Khan, S. A., Aschwanden, A., Bjørk, A. A., Wahr, J., Kjeldsen, K. K., and Kjær, K. H.: Greenland ice sheet mass balance: a review, Rep. Prog. Phys., 78, 046801, doi:10.1088/0034-4885/78/4/046801, 2015.
Kimura, S., Holland, P. R., Jenkins, A., and Piggott, M.: The effect of meltwater plumes on the melting of a vertical glacier face, J. Phys. Oceanogr., 44, 3099–3117, doi:10.1175/JPO-D-13-0219.1, 2014.
Krabill, W., Abdalati, W., Frederick, E., Manizade, S., Martin, C., Sonntag, J., Swift, R., Thomas, R., Wright, W., and Yungel, J.: Greenland ice sheet: high-elevation balance and peripheral thinning, Science, 289, 428–430, doi:10.1126/science.289.5478.428, 2000.
Krabill, W. B.: IceBridge ATM L2 Icessn Elevation, Slope, and Roughness, [1993–2014], NASA Distributed Active Archive Center at the National Snow and Ice Data Center, Boulder, Colorado, USA, Digital media, Updated 2014, available at: http://nsidc.org/data/ilatm2.html (last access: 10 September 2015), 2014.
Larour, E., Seroussi, H., Morlighem, M., and Rignot, E.: Continental scale, high order, high spatial resolution, ice sheet modeling using the Ice Sheet System Model (ISSM), J. Geophys. Res.-Earth, 117, F01022, doi:10.1029/2011JF002140, 2012.

TCD
9, 4865–4892, 2015

Levermann, A., Albrecht, T., Winkelmann, R., Martin, M. A., Haseloff, M., and Joughin, I.: Kinematic first-order calving law implies potential for abrupt ice-shelf retreat, The Cryosphere, 6, 273–286, doi:10.5194/tc-6-273-2012, 2012.
Luckman, A. and Murray, T.: Seasonal variation in velocity before retreat of Jakobshavn Isbræ, Greenland, J. Geophys. Res. Lett., 32, L08501, doi:10.1029/2005GL022519, 2005.
MacAyeal, D. R., Scambos, T. A., Hulbe, C. L., and Fahnestock, M. A.: Catastrophic iceshelf break-up by an ice-shelf-fragment-capsize mechanism, J. Glaciol., 49, 22–36, 2003.
Martin, M. A., Winkelmann, R., Haseloff, M., Albrecht, T., Bueler, E., Khroulev, C., and Levermann, A.: The Potsdam Parallel Ice Sheet Model (PISM-PIK) – Part 2: Dynamic equilibrium simulation of the Antarctic ice sheet, The Cryosphere, 5, 727–740, doi:10.5194/tc-5-727-2011, 2011.
Mengel, M. and Levermann, A.: Ice plug prevents irreversible discharge from East Antarctica, Nature Clim. Change, 4, 451–455, doi:10.1038/nclimate2226, 2014.
Moon, T., Joughin, I., Smith, B., and Howat, I.: 21st-Century evolution of Greenland outlet glacier velocities, Science, 336, 576–578, doi:10.1126/science.1219985, 2012.
Motyka, R. J., Truffer, M., Fahnestock, M., Mortensen, J., Rysgaard, S., and Howat, I.: Submarine melting of the 1985 Jakobshavn Isbræ floating tongue and the triggering of the current retreat, J. Geophys. Res., 116, F01007, doi:10.1029/2009JF001632, 2011.
NSIDC: 2014 melt season in review, National Snow and Ice Data Center (NSIDC), available at: http://nsidc.org/greenland-today/2015/01/2014-melt-season-in-review/ (last access: 9 July 2015), 2015.
Nghiem, S. V., Hall, D. K., Mote, T. L., Tedesco, M., Albert, M. R., Keegan, K., Shuman, C. A., DiGirolamo, N. E., and Neumann, G.: The extreme melt across the Greenland ice sheet in 2012, Geophys. Res. Lett., 39, L20502, doi:10.1029/2012GL053611, 2012.
Nick, F. M., Vieli, A., Howat, I. M., and Joughin, I.: Large-scale changes in Greenland outlet glacier dynamics triggered at the terminus, Nat. Geosci., 2, 110–114, doi:10.1038/ngeo394, 2009.
Nick, F. M., Vieli, A., Andersen, M. L., Joughin, I., Payne, A., Edwards, T. L., Pattyn, F., and van de Wal, R. S.: Future sea-level rise from Greenland's main outlet glaciers in a warming climate, Nature, 497, 235–238, doi:10.1038/nature12068, 2013.
Nielsen, K., Khan, S. A., Spada, G., Wahr, J., Bevis, M., Liu, L., and van Dam, T.: Vertical and horizontal surface displacements near Jakobshavn Isbræ driven by melt-induced and dynamic ice loss, J. Geophys. Res.-Sol. Ea., 118, 1837–1844, doi:10.1002/jgrb.50145, 2013.

TCD
9, 4865–4892, 2015
Glacier dynamics over the last quarter of a century at Jakobshavn Isbræ
I. S. Muresan et al.

Noël, B., van de Berg, W. J., van Meijgaard, E., Kuipers Munneke, P., van de Wal, R. S. W., and van den Broeke, M. R.: Summer snowfall on the Greenland Ice Sheet: a study with the updated regional climate model RACMO2.3, The Cryosphere Discuss., 9, 1177–1208, doi:10.5194/tcd-9-1177-2015, 2015.

Parizek, B. R. and Walker, R. T.: Implications of initial conditions and ice–ocean coupling for grounding-line evolution, Earth Planet. Sc. Lett., 300, 351–358, doi:10.1016/j.epsl.2010.10.016, 2010.

Pattyn, F., Schoof, C., Perichon, L., Hindmarsh, R. C. A., Bueler, E., de Fleurian, B., Durand, G., Gagliardini, O., Gladstone, R., Goldberg, D., Gudmundsson, G. H., Huybrechts, P., Lee, V., Nick, F. M., Payne, A. J., Pollard, D., Rybak, O., Saito, F., and Vieli, A.: Results of the Marine Ice Sheet Model Intercomparison Project, MISMIP, The Cryosphere, 6, 573–588, doi:10.5194/tc-6-573-2012, 2012.

Pollard, D., DeConto, R. M., and Alley, R. B.: Potential Antarctic Ice Sheet retreat driven by hydrofracturing and ice cliff failure, Earth Planet. Sc. Lett., 412, 112–121, doi:10.1016/j.epsl.2014.12.035, 2015.

Price, S. F., Payne, A. J., Howat, I. M., and Smith, B. E.: Committed sea-level rise for the next century from Greenland ice sheet dynamics during the past decade, P. Natl. Acad. Sci. USA, 108, 8978–8983, doi:10.1073/pnas.1017313108, 2011.

Rignot, E., Bamber, J. L., van den Broeke, M. R., Davis, C., Li, Y., van de Berg, W. J., and van Meijgaard, E.: Recent Antarctic ice mass loss from radar interferometry and regional climate modeling, Nat. Geosci., 1, 106–110, doi:10.1038/ngeo102, 2008.

Schoof, C: Ice sheet grounding line dynamics: steady states, stability, and hysteresis, J. Geophys. Res., 112, F03S28, doi:10.1029/2006JF000664, 2007.

Seroussi, H., Dhia, H. B., Morlighem, M., Larour, E., Rignot, E., and Aubry, D.: Coupling ice flow models of varying orders of complexity with the Tiling method, J. Glaciol., 58, 776–786, doi:10.3189/2012JoG11J195, 2012.

Shapiro, N. M. and Ritzwoller, M. H.: Inferring surface heat flux distributions guided by a global seismic model: particular application to Antarctica, Earth Planet. Sc. Lett., 223, 213–224, doi:10.1016/j.epsl.2004.04.011, 2004.

Shepherd, A., Ivins, E. R., Geruo, A., Barletta, V. R., Bentley, M. J., Bettadpur, S., Briggs, K. H., Bromwich, D. H., Forsberg, R., Galin, N., Horwath, M., Jacobs, S., Joughin, I., King, M. A., Lenaerts, J. T. M., Li, J., Ligtenberg, S. R. M., Luckman,A., Luthcke, S. B., McMillan, M., Meister, R., Milne, G., Mouginot, J., Muir, A., Nicolas, J. P., Paden, J., Payne, A. J., Pritchard, H., Rignot, E., Rott,H., Sørensen, L. S., Scambos, T. A., Scheuchl, B., Schrama, E. J. O., Smith, B., Sundal, A. V., van Angelen, J. H., van de Berg, W. J., van den Broeke, M. R., Vaughan, D. G., Velicogna, I., Wahr, J., Whitehouse, P. L., Wingham, D. J., Yi, D., Young, D., and Zwally, H. J.: A reconciled estimate of ice-sheet mass balance, Science, 338, 1183–1189, doi:10.1126/science.1228102, 2012.

Slater, D. A., Nienow, P. W., Cowton, T. R., Goldberg, D. N., and Sole, A. J.: Effect of near-terminus subglacial hydrology on tidewater glacier submarine melt rates, Geophys. Res. Lett., 42, 2861–2868, doi:10.1002/2014GL062494, 2015.

Smith, B., Howat, I., Moon, T., Scambos, T., and Joughin, I.: Greenland flow variability from ice-sheet-wide velocity mapping, J. Glaciol., 56, 415–430, 2010.

Stanley, S. J., Jenkins, A., Giulivi, C. F., and Dutrieux, P.: Stronger ocean circulation and increased melting under Pine Island Glacier ice shelf, Nat. Geosci., 4, 519–523, doi:10.1038/ngeo1188, 2011.

Tedesco, M., Fettweis, X., Mote, T., Wahr, J., Alexander, P., Box, J. E., and Wouters, B.: Evidence and analysis of 2012 Greenland records from spaceborne observations, a regional climate model and reanalysis data, The Cryosphere, 7, 615–630, doi:10.5194/tc-7-615-2013, 2013.

The PISM Authors: PISM, a Parallel Ice Sheet Model, User's Manual, available at: http://www.pism-docs.org/wiki/lib/exe/fetch.php?media=manual.pdf (last access: 15 June 2015), 2014.

Thomas, H. R., Abdalati, W., Frederick, E., Krabill, W. B., Manizade, S., and Steffen, K.: Investigation of surface melting and dynamic thinning on Jakobshavn Isbræ, J. Glaciol., 49, 231–239, doi:10.3189/172756503781830764, 2003.

Thomas, R. H.: Force-perturbation analysis of recent thinning and acceleration of Jakobshavn Isbrae, Greenland, J. Glaciol., 50, 57–66, doi:10.3189/172756504781830321, 2004.

van den Broeke, M., Bamber, J., Ettema, J., Rignot, E., Schrama, E., van de Berg, W. J., van Meijgaard, E., Velicogna, I., and Wouters, B.: Partitioning recent Greenland mass loss, Science, 326, 984–986, doi:10.1126/science.1178176, 2009.

Van der Veen, C. J., Plummer, J. C., and Stearns, L. A.: Controls on the recent speed-up of Jakobshavn Isbræ, West Greenland, J. Glaciol., 57, 770–782, 2011.

Vieli, A. and Nick, F. M.: Understanding and modeling rapid dynamic changes of tidewater outlet glaciers: issues and implications, Surv. Geophys., 32, 437–458, doi:10.1007/s10712-011-9132-4, 2011.

TCD

9, 4865–4892, 2015

Winkelmann, R., Martin, M. A., Haseloff, M., Albrecht, T., Bueler, E., Khroulev, C., and Levermann, A.: The Potsdam Parallel Ice Sheet Model (PISM-PIK) Part 1: Model description, The Cryosphere, 5, 715–726, doi:10.5194/tc-5-715-2011, 2011.

TCD
9, 4865–4892, 2015

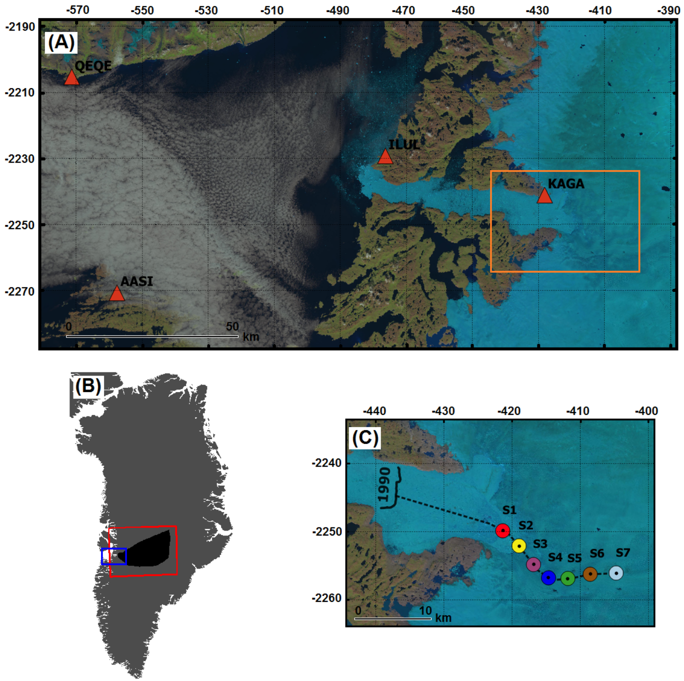

Figure 1. (a) Landsat 8 image of Ilulissat fjord and part of Disko Bay acquired in August 2014. The dark orange triangles indicate the GPS station locations (GPS data shown in Fig. 5). The polygon defined by light orange borders outlines the location of **(c)**. **(b)** Grey filled Greenland contour map. The black filled polygon highlights the JI basin used to compute the mass loss (Fig. 4) and is identical to Khan et al., 2014. The polygon defined by red borders indicates the computational domain. The blue border polygon represents the location of **(a)**. **(c)** Coloured circles indicate the locations plotted in Fig. 3. The thick black line denotes the JI terminus position in 1990s. The dotted black line represents the flow-line location plotted in Fig. 6. The coordinates given outside defining the image gridding **(a)** and **(c)** are in polar-stereographic projection units (km).

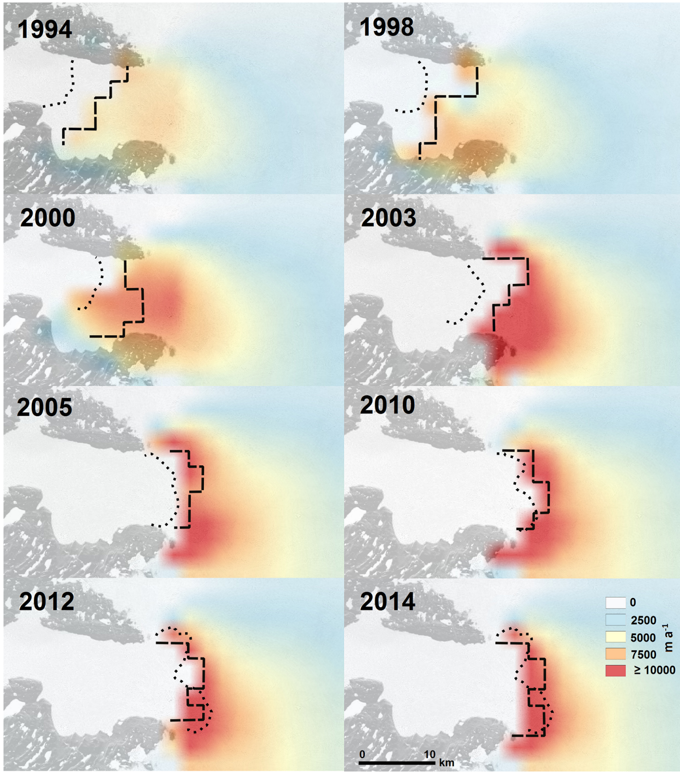

Figure 2. Modelled velocities at Jakobshavn Isbræ for December are shown for seven different years. The black dotted line denotes the observed front position and the thick black dashed line represents the modelled grounding line position. The velocities are displayed over a Landsat 8 image acquired in August 2014.

TCD
9, 4865–4892, 2015
Glacier dynamics over the last quarter of a century at Jakobshavn Isbræ
I. S. Muresan et al.

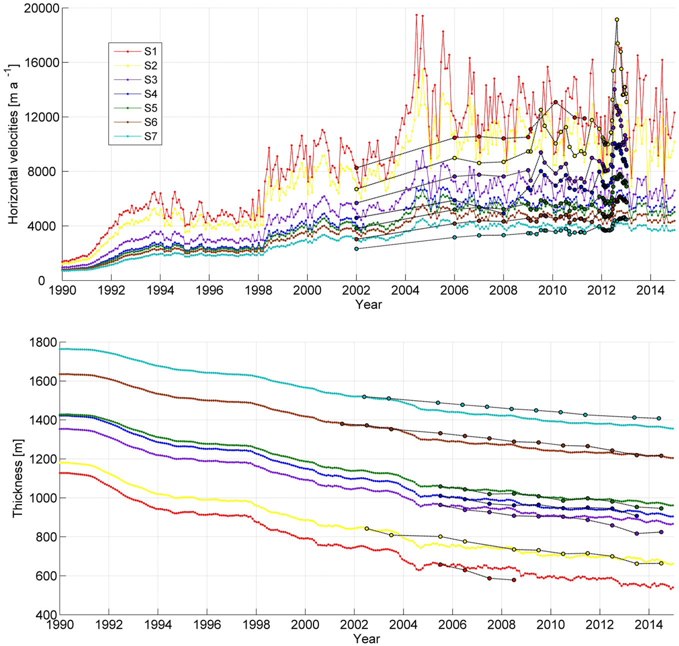

Figure 3. Time series of modelled (filled circles) vs. observed (filled circles with black edges) velocities (Smith et al., 2010) (top figure) and ice thickness changes (Krabill, 2014) (bottom figure) for the period 1990-2014 at the point locations (S1 to S7) shown in Fig. 1c. The same colour scheme is used for the modelled and the observed data.

TCD
9, 4865–4892, 2015

Glacier dynamics over the last quarter of a century at Jakobshavn Isbræ

I. S. Muresan et al.

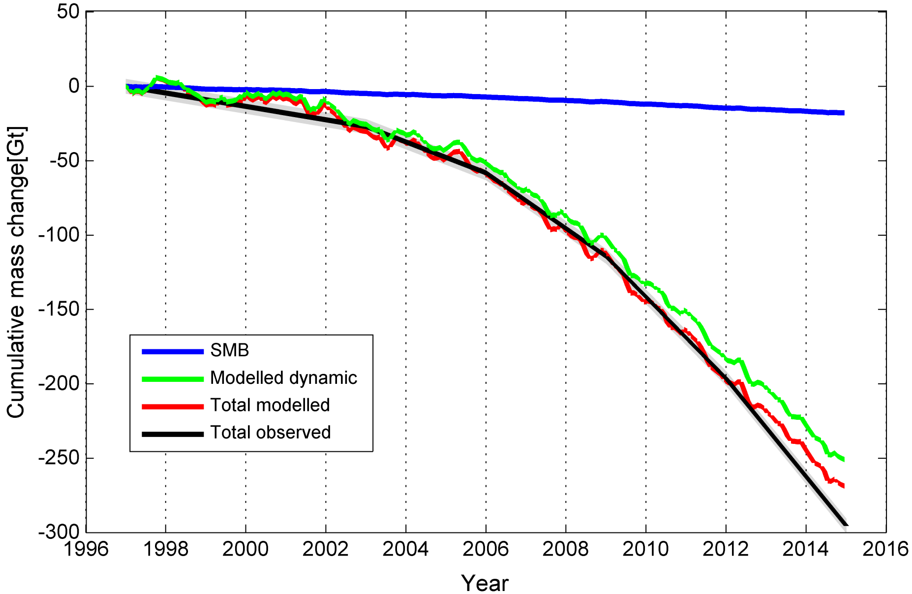

Figure 4. Modelled and observed cumulative mass change for Jakobshavn Isbræ. The blue curve represents the mass change due to the SMB variability after the 1960–1990 baseline is removed. The green curve represents the modelled ice dynamics mass change. To estimate the mass change due to changes in ice dynamics, we subtract the SMB mass change (as calculated based on RACMO 2.3, Noël et al., 2015) from the total modelled mass change. The red curve represents the total modelled mass change including both SMB and ice dynamic changes. The black curve with grey error limits represents the total observed mass change including both SMB and ice dynamic changes. The modelled mass change for the period 1997–2014 is ~ 269 Gt and the observed mass change is ~ 296 Gt.

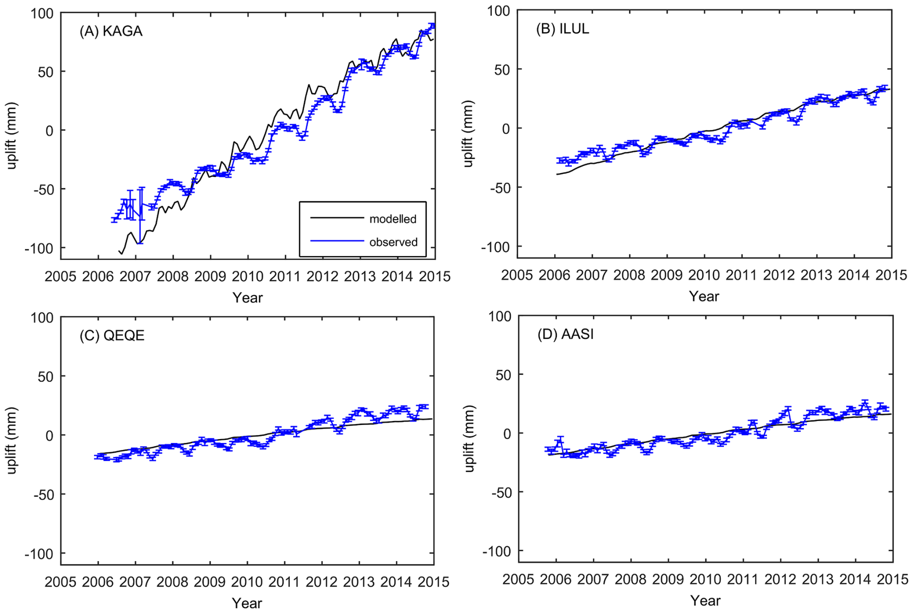

Figure 5. Observed vs. modelled uplift in mm for the stations KAGA **(a)**, ILUL **(b)**, QEQE **(c)** and AASI **(d)**. The positions of the four GPS stations are presented in Fig. 1a.

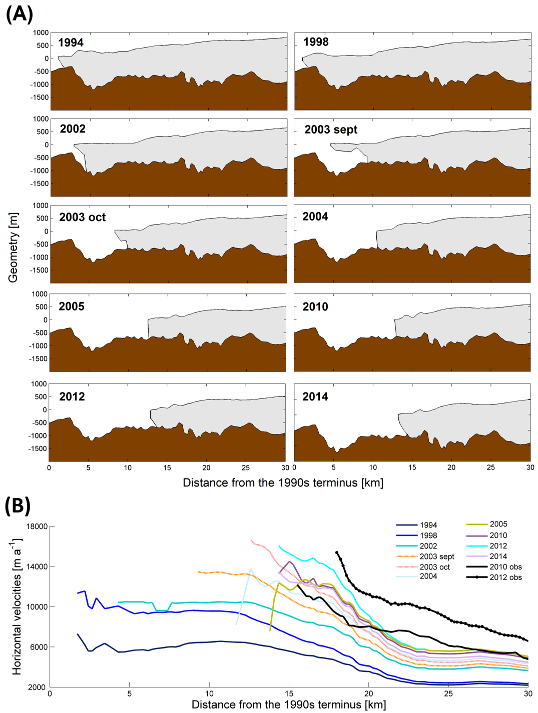

Figure 6. Modelled evolution of surface elevation **(a)** and horizontal velocities **(b)** of Jakobshavn Isbræ for December along the flow-line shown in Fig. 1c. Note the acceleration in speed **(b)** between September 2003 (orange) and October 2003 (light pink) corresponding to the final breakup of the floating tongue. The black lines in **(b)** denote observed horizontal velocities as produced from TerraSAR-X (TSX) image pairs collected between 20 November 2010–1 December 2010 and 8 December 2012–19 December 2012 (Joughin et al., 2010, 2011).

TCD
9, 4865–4892, 2015